

ОПРЕДЕЛЕНИЕ ТЕМПЕРАТУРНОГО РЕЖИМА РАБОТЫ СКВАЖИН, ОБОРУДОВАННЫХ УЭЦН, И ОЦЕНКА ВЕРОЯТНОСТИ ОСЛОЖНЕНИЙ ПРИ ВЫХОДЕ НАСОСНОЙ УСТАНОВКИ ИЗ ОПТИМАЛЬНОЙ ТЕМПЕРАТУРНОЙ ЗОНЫ

М. В. Шаронов¹, О. А. Грибенников²

¹ Самарский государственный технический университет, Самара, Россия

² Самарский научно-исследовательский и проектный институт нефтедобычи ООО «СамараНИПИНефть», Самара, Россия

Аннотация: описана методика, позволяющая рассчитать температуру на приеме насоса в зависимости от технологического режима работы добывающих скважин и продемонстрировано ее применение на примере фонда добывающих скважин АО «Самаранефтегаз». Повышение температуры рассчитывается с учетом наличия свободного газа в корпусе насосного оборудования. Такой рост негативно сказывается на работе насосной установки в целом, так как существуют риски перегрева кабельной линии в нижних секциях насоса и образования неорганических отложений в самом насосе.

Ключевые слова: газовый фактор, газосодержание, ЭЦН, электроцентробежный насос, нефтяная скважина, рост температуры, осложнения при добыче

Для цитирования: Шаронов М. В., Грибенников О. А. Определение температурного режима работы скважин, оборудованных УЭЦН, и оценка вероятности осложнений при выходе насосной установки из оптимальной температурной зоны // Горный информационно-аналитический бюллетень. – 2022. – № 10-2. – С. 71–77. DOI: 10.25018/0236_1493_2022_102_0_71.

Determination of the temperature operation mode of wells equipped with ESPs and assessment of the probability of complications when the pump unit leaves the optimal temperature zone

M. V. Sharonov¹, O. A. Gribennikov²

¹ Samara State Technical University, Samara, Russia;

² Samara's Petroleum Research Institute LLC "SamaraNIPIneft", Samara, Russia

Abstract: This article describes the methodology that allows to calculate the temperature at the pump intake depending on the technological mode of producing wells and demonstrates its application by the example of the stock of producing wells of Samaraneftgaz AO. The temperature increase is calculated taking into account the presence of free gas in the pumping equipment chamber. Such increase negatively affects the operation of the unit as a whole, since there are risks of overheating the cable line in the lower sections of the pump and scale formation in the pump itself.

Key words: Gas-Oil Ratio, Gas Content, ESP, Electrical Submersible Pump, Oil Well, Temperature Increase, Scaling, Production Problems.

For citation: Sharonov M. V., Gribennikov O. A. Determination of the temperature operation mode of wells equipped with ESPs and assessment of the probability of complications when the pump unit leaves the optimal temperature zone. *MIAB. Mining Inf. Anal. Bull.* 2022;(10-2):71–77. [In Russ]. DOI: 10.25018/0236_1493_2022_102_0_71.

1 Introduction

Operation of electric submersible units is associated with complications leading to failures. The most common cause of failure is overheating and deposition of inorganic salts, which occur as a result of intensive heat release, the amount of which exceeds the heat dissipation by the well products [1–7]. When operating ESPs at high temperatures, the MTBF (mean time between failures) decreases dramatically, and the probability of the inorganic salt depositing on the moving parts of the ESPs increases [8–12], resulting in failure of the pump unit [13, 14]. In some cases, the elevated temperatures can lead to melting of the cable lines insulation [15]. Abnormal temperature conditions are most pronounced in wells with high gas-oil ratio and low flow rate, as well as in wells with bottomhole pressure significantly below the bubble-point (saturation) pressure [1, 14, 16]. Such operating conditions are characteristic of many wells in the fields of the Samaraneftgaz AO.

In Samaraneftgaz AO, the main share of production wells equipped with artificial lift systems at the beginning of 2021 is operated by electric submersible pump units (ESPs) (Fig. 1).

Knowledge of the temperature operating mode as a function of many variables would allow preventive measures to optimize the operation of such wells, increase the average time between failures, and improve the technical and economic performance of wells, reducing operating and maintenance costs.

2 Calculation methodology

To estimate the thermal state of the fluid flow, it is necessary to calculate the temperature in the pump, taking into account the free gas content in the flow. The temperature in the pump was calculated by the formula [17]:

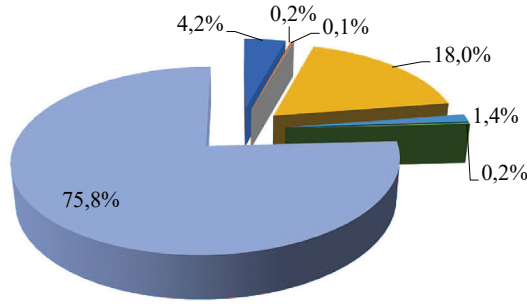
$$T_w = T_f + \Delta T_w = T_f + \frac{P_{sat} + C_1 \theta \cdot \Delta x}{\frac{1}{C_2} - C_1}, \quad (1)$$

where T_w – pump casing temperature, K; T_f – temperature of the gas-liquid mixture at the pump intake, K; ΔT_w – temperature increase between the point of the pump intake and the point of the complete gas dissolution inside the pump, K; P_{sat} – bubble-point (saturation) pressure, atm; C_1 – coefficient accounting for the change in saturation pressure from temperature, atm/K; θ – geothermal gradient in the well, K/m; Δx – distance from the upper perforation holes to the pump, m; C_2 – a constant value added to simplify calculations, atm/K.

In this study, the geothermal gradient θ was taken as 0.0357 K/m, T_f was taken on average 10°K above the reservoir temperature, since the fluid flow is heated by the submersible motor by about 5–15°K.

C_1 is calculated by the following formula:

$$C_1 = \frac{1}{9,157 + \frac{701,8}{G_f(y_m - 0,8y_n)}}, \quad (2)$$



■ Swabbing ■ Flowing ■ SRSP ■ SRP ■ ESP (screw) ■ EDP ■ ESP

Fig. 1. Distribution of the Samaraneftgaz AO production well stock by methods of operation method as of the beginning of 2021

where G_f is the gas-oil ratio, m^3/t ; y_m , y_n – content of methane and nitrogen in the gas fraction, respectively, C_2 is calculated as follows:

$$C_2 = \frac{\phi}{1 - \phi} \frac{q_0 R_2 P_{int}}{2(1 - B)hGP_{atm}} \left\{ \frac{1}{\alpha} + \frac{\delta_{gl}}{\lambda_{gl}} \right\}, \quad (3)$$

where ϕ – free gas content in the mixture, fraction; q_0 – heat source power density, W/m^3 ; R_2 – radius of the cylindrical pump casing, m; P_{int} – pump intake pressure, atm; δ_{gl} – size of gas bubbles at the pump intake, m (taken equal 0.001 m); λ_{gl} – thermal conductivity of gas layer on the surface of the casing (we take it as 5), $W/(m \cdot K)$; B – water content in the well production, fraction; h – pump head, m; G – formation gas-oil ratio, m^3/m^3 ; P_{atm} – atmospheric pressure, atm; α – convective heat transfer coefficient (we take it as 3800), $W/(m^2 \cdot K)$.

The actual free gas content in the mixture ϕ is determined by the expression:

$$\phi = \frac{\beta_{sat}}{1 + \beta_{sat} \frac{C_b}{C}}, \quad (4)$$

where β_{sat} – gas content in the pump, fraction; C_b – gas bubble rise velocity, depending on water content in the well

production, m/s (at $B < 0.5 C_{sat} = 0.02$ m/s, at $B \geq 0.5 C_{sat} = 0.16$ m/s); C – effective gas speed in the casing section at the pump intake, m/s.

To determine the gas content of the pump, the gas content at the pump intake and the gas separation factor must be determined. The gas content at the pump intake is calculated according to the following expression:

$$\beta_{int} = \frac{G_{int}}{(1 + P_{int})B^* + 1}, \quad (5)$$

where G_{int} – free gas volume at the pump intake, m^3/t ; P_{int} – pressure at the pump intake, Pa; B^* – oil formation volume factor at pressure at the pump intake.

Free gas volume at the pump intake G_{int} is calculated by the expression (6):

$$G_{int} = G_f \left[1 - \frac{P_{int}}{P_{sat}} \right], \quad (6)$$

where G_f – gas-oil ratio, m^3/t ; P_{int} and P_{sat} are pressure at the pump intake and pressure bubble-point (saturation), respectively, Pa.

The oil formation volume factor B^* at pump intake pressure is calculated by the expression:

$$B^* = B + (1 - B) \left[1 + (b - 1) \sqrt{\frac{P_{int}}{P_{sat}}} \right], \quad (7)$$

where b is the oil formation volume factor at the pressure of saturation.

The gas content in the pump including gas separation is determined by the following expression:

$$\beta_{pump} = \beta_{int} (1 - K_s), \quad (8)$$

The separation coefficient is calculated by the formula [1]:

$$K_s = K_{ns} + K_{gsi} (1 - K_{ns}), \quad (9)$$

where K_{gsi} is the gas separation coefficient with a gas separator coefficient (if the separator is present in the assembly, it is taken in calculations equal to 0.85, if not – 0 [18]), fraction.

K_{ns} , the natural gas separation coefficient at the intake of the submersible pump, is calculated by the formula [19]:

$$K_{ns} = \frac{1}{1 + \frac{6.02 Q_{int}}{f_{well2}}}, \quad (10)$$

where f_{well2} is the area of the annulus formed by the inner surface of the casing and the pump housing, m^2 .

The effective gas velocity in the casing cross-section at the pump intake C is calculated as

$$C = \frac{Q_{g.int}}{f_{well}}, \quad (11)$$

where $Q_{g.int}$ is the volumetric gas flow rate at the pump intake, m^3/s ; f_{well} is the cross-sectional area of the well at the pump intake, m^2 .

The volumetric gas flow rate at the pump intake $Q_{g.int}$ is calculated as follows:

$$Q_{g.int} = \frac{Q_{int} \beta_{int}}{1 - \beta_{int}}, \quad (12)$$

where Q_{int} is the volumetric fluid flow rate at the pump intake, m^3/s .

The volumetric fluid flow rate at the pump intake is related to the oil formation fluid factor at the pump intake pressure by the following equation:

$$Q_{int} = Q \cdot B^*, \quad (13)$$

where Q is the fluid flow rate, m^3/s .

The heat source power density q_0 is defined as

$$q_0 = \frac{q}{V_1} = \frac{q}{\pi R^2 l}, \quad (14)$$

where q is the heat source power of one ESP stage, W ; V_1 is the volume of one ESP stage, m^3 ; R is the radius of the cylindrical pump casing, m ; l is the pump stage's height, m .

The heat source power of one ESP stage is defined by the following equation:

$$q = \frac{Q_p}{n_{stages}}, \quad (15)$$

where Q_p is the power, consumed by the pump to produce heat, W ; n_{stages} is the number of stages in the pump.

The power, consumed by the pump to produce heat is determined by the following expression:

$$Q_p = N_{SEM} \cdot \eta_{SEM} \cdot (1 - \eta_{pump}), \quad (16)$$

where N_{SEM} is the power of the submersible electric motor, W ; η_{SEM} is the submersible motor efficiency, fraction; η_{pump} is the pump efficiency at current capacity, fraction.

If a TMS (downhole telemetry system) is installed on the pump unit, the pump intake pressure value P_{int} is taken from the data provided by the sensor, otherwise it is defined from the expression:

$$P_{int} = P_{casing} + (H_{pump} - H_{DFL}) \bar{\rho}_O g \cdot 10^{-5}, \quad (17)$$

where P_{casing} is the annular pressure, atm ; $\bar{\rho}_O$ is the average oil density, kg/m^3 ; H_{pump} is the pump depth of immersion, m ; H_{DFL} is the dynamic fluid level, m ; g is the acceleration of gravity, m/s^2 .

Calculations of cable line temperatures upstream of the pump were carried out for the producing well stock of the Samaraneftgaz AO. The calculations involved 558 wells. Equipment data from pump manufacturers were used in the calculations [20–22].

The following restrictions were imposed on the wells, for which the calculations were carried out:

1. The well is operated by ESP;
2. The well is operated continuously;
3. The well is developing a single reservoir;
4. Russian-made ESP is installed on the well to determine pump characteristics
5. There is no packer in the well.

Five ranges were chosen for the analysis. In the wells where the temperature upstream of the pump does not exceed 90°C, there is no intensive salt deposition and there are no problems with overheating and melting of the cable line insulation upstream of the pump. At temperatures above 90°C, the solubility of inorganic salts such as calcite, barite, anhydrite and gypsum decreases and thus the well and the pump show signs of scaling [10–12, 23].

At about 120°C, there will be signs of overheating of the cable line (provided that the cable extension has an operating temperature limit of 120°C) [24, 25]. In the temperature range from 120 to 160°C, the well will also show signs of scaling, and there is a possibility overheating the cable line if the cable line extension has an operating temperature limit of 160°C [24, 25], or melting if the cable line extension has an operating temperature limit of 120°C. If the ESP operates above 160°C, the main problem will be melting of the cable extension (drop in the cable line insulation resistance to 0), unless a temperature-resistant extension cord designed to operate at temperatures up to 230°C is used [24, 25]. The results of calculating the temperature distribution of the cable line upstream the pump for the stock of production wells equipped with ESPs (558 units) are shown in Fig. 2.

As shown in Fig. 2, most wells (397 units) operate in the optimal temperature range with temperatures below 90°C. Fifty-three wells are at risk of scaling. A total of 108 wells are at risk of melting the cable line upstream of the pump and scaling.

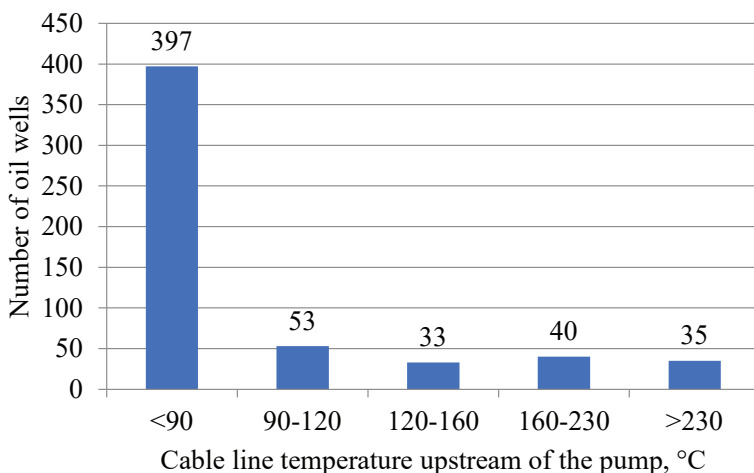


Fig. 2. Distribution of the well stock according to the calculated temperature of the cable line upstream the pump

Thus, 161 wells (29% of the stock of production wells equipped with ESPs) experience complications caused by scaling or melting in the cable line due to insufficient cooling of the ESP motor and overheating. Early detection of the wells working in a suboptimal temperature mode will allow taking preventive measures to prevent failures, increase the MTBF, and improve technical and economic performance

of the stock. The developed software, working with the technological mode of production wells of Samarneftegaz AO and capable to be integrated into it, will allow conducting tests to identify wells operating in suboptimal temperature mode.

It is also recommended to add to the technological mode a column with the cable temperature upstream the pump and the gas content at the pump intake.

REFERENCES

1. Drozdov, A. N. (2008). Technology and technique of oil production by submersible pumps in complicated conditions. Moscow: MAKS Press.
2. Gizatullin, F. A., Khakimyanov, M. I., Shafikov, I. N. (2019). Energy efficiency of well electric submersible pumps for oil production. IOP Conference Series: Materials Science and Engineering, 537(6), 062006. DOI: 10.1088/1757-899X/537/6/062006.
3. Oliva, G. B., Galvao, H. L., Dos Santos, D. P., et al. (2017). Gas Effect in Electrical-Submersible-Pump-System Stage-by-Stage Analysis. SPE Production & Operations, 32(03), 294–304. DOI: 10.2118/173969-PA.
4. Abbariki, G., Riasi, A., Rezghi, A. Surrogate-Based Optimization for the Design of Rotary Gas Separator in ESP Systems. SPE Production & Operations, 35(03), 497–509. DOI: 10.2118/201188-PA.
5. Zhu, J., Zhang, J., Cao, G., et al. (2019). Modeling flow pattern transitions in electrical submersible pump under gassy flow conditions. Journal of Petroleum Science and Engineering, 180, 471–484.
6. Dupoirion, M. (2018). Experimental Study of Gas-Liquid Flow Through a Multi-Stage, Mixed-Flow Electric Submersible Pump. Proceedings of the ASME 2018 5th Joint US-European Fluids Engineering Division Summer Meeting, 3, V003T12A005. DOI: 10.1115/FEDSM2018-83032.
7. Martins, J. R., Ribeiro, D. C., Pereira, F. A., et al. (2020). Heat dissipation of the Electrical Submersible Pump (ESP) installed in a subsea skid. Oil & Gas Science and Technology – Revue d'IFP Energies nouvelles, 75, 13.
8. Cosmo, R. P., Ressel Pereira, F. A., Ribeiro, D. C., et al. (2019). Estimating CO₂ degassing effect on CaCO₃ precipitation under oil well conditions. Journal of Petroleum Science and Engineering, 181, 106207.
9. Droguett, E. L., Lins, I. D., Moura, M. C., et al. (2015). Variable selection and uncertainty analysis of scale growth rate under pre-salt oil wells conditions using support vector regression. Journal of Risk and Reliability, 229(4), 319–326.
10. Gareev, A. A. (2021). Salt Deposition in Electric Submersible Centrifugal Pumps under Intermittent Operation. Petroleum & Petrochemical Engineering Journal, 5(2), 1–6.
11. Gareev, A. A. (2018). On the issue of predicting scale in installations of electric centrifugal pumps. Equipment and technologies for the oil and gas complex, 5, 37–42.
12. Saychenko, L., Tananykhin, D., Ashena, R. (2021). Prevention of scale in the downhole equipment and productive reservoir during the oil well operation. Journal of Applied Engineering Science, 19(2), 363–368.
13. Fakher, S., Khlaifat, A., Hossain, M., et al. (2021). Rigorous review of electrical submersible pump failure mechanisms and their mitigation measures. Journal of Petroleum Exploration and Production Technology, 11, 3799–3814.

14. Ricardo, D. M., Jiménez, G. E., Ferreira, J. V., et al. (2018). Multiphase gas-flow model of an electrical submersible pump. *Oil & Gas Science and Technology – Revue d'IFP Energies nouvelles*, 73, 29.

15. Suleimanov, R. I., Khabibullin, M. Ya. (2019). Analysis of the reliability of the power cable of an electric-centrifugal pump unit. *IOP Conference Series: Earth and Environmental Science*, 378, 012054.

16. Bremner, C., Harris, G., Kosmala, A., et al. (2016). Evolving technologies: electrical submersible pumps. *Oilfield Review*, 18(4), 30–43.

17. Gareev, A. A. (2010). About the temperature regime of the electric submersible pump. *Equipment and technologies for oil and gas complex*, 6, 35–41.

18. Drozdov, A. N. (2011). ESP with and without gas separator: rationality. *Neftegazovaya Vertikal'*, 13–14, 128–129.

19. Mishchenko, I. T. (2015). *Oil production from wells*. Moscow: Gubkin Russian State University of Oil and Gas Publishing Center.

20. *Catalog oborudovaniya Borets* (2012).

21. *Catalog oborudovaniya GK Novomet-Perm* (2009).

22. *Catalog pogruzhnogo oborudovaniya UETsN TPS-LINE «Schlumberger»* (2015).

23. Brahmi, H. (2018). Lessons Learned from Electrical Submersible Pumps Installed in High-Salinity and Corrosive Reservoir, TAGI Formation. *SPE Production & Operations*, 33(04), 913–927.

24. *Catalog “Cabels for UETsN” OOO NPK Energiya* (2019).

25. Ismailov, G. M., Tyurin, A. E., Pavlov, M. S., et al. (2018). Strength Problems of Submersible Pump Power Cables in the Oil Industry. *AIP Conference Proceedings*, 2053, 040033. **PLoS**

ИНФОРМАЦИЯ ОБ АВТОРАХ

*Шаронов Максим Владиславович*¹ – магистрант кафедры разработки и эксплуатации нефтяных и газовых месторождений,

e-mail: volgamiddle@yandex.ru,

ORCID ID: 0000-0003-1845-2542;

*Грибенников Олег Алексеевич*² – канд. техн. наук, доцент, главный специалист,

e-mail: o.a.gribennikov@mail.ru,

ORCID ID: 0000-0003-3286-6979;

¹ Самарский государственный технический университет;

² Самарский научно-исследовательский и проектный институт нефтедобычи ООО «СамараНИПИНефть».

Для контактов: *Шаронов М. В.*, e-mail: volgamiddle@yandex.ru.

INFORMATION ABOUT THE AUTHORS

*Sharonov M. V.*¹, MSc. (Eng.), Researcher,

e-mail: volgamiddle@yandex.ru,

ORCID ID: 0000-0003-1845-2542;

*Gribennikov O. A.*², Cand. Sci. (Eng.), Chief specialist,

e-mail: o.a.gribennikov@mail.ru,

ORCID ID: 0000-0003-3286-6979;

¹ Samara State Technical University, 443100, Samara, Russia;

² Samara's Petroleum Research Institute LLC «SamaraNIPIneft», 443096 Samara, Russia.

Corresponding author: *Sharonov M. V.*, e-mail: volgamiddle@yandex.ru.

Получена редакцией 20.03.2022; получена после рецензии 15.07.2022; принята к печати 10.09.2022.

Received by the editors 20.03.2022; received after the review 15.07.2022; accepted for printing 10.09.2022.